

complication in 19–20% of patients (Johnson, 2009). These effects have been associated

Table 1

Equilibria of the migration model (6)–(7) and their stability. All solutions are finite as long as $df \neq 1$, which we assume here. The stability criteria are identified in Appendix D. Entries with a dash (-) are omitted here due to

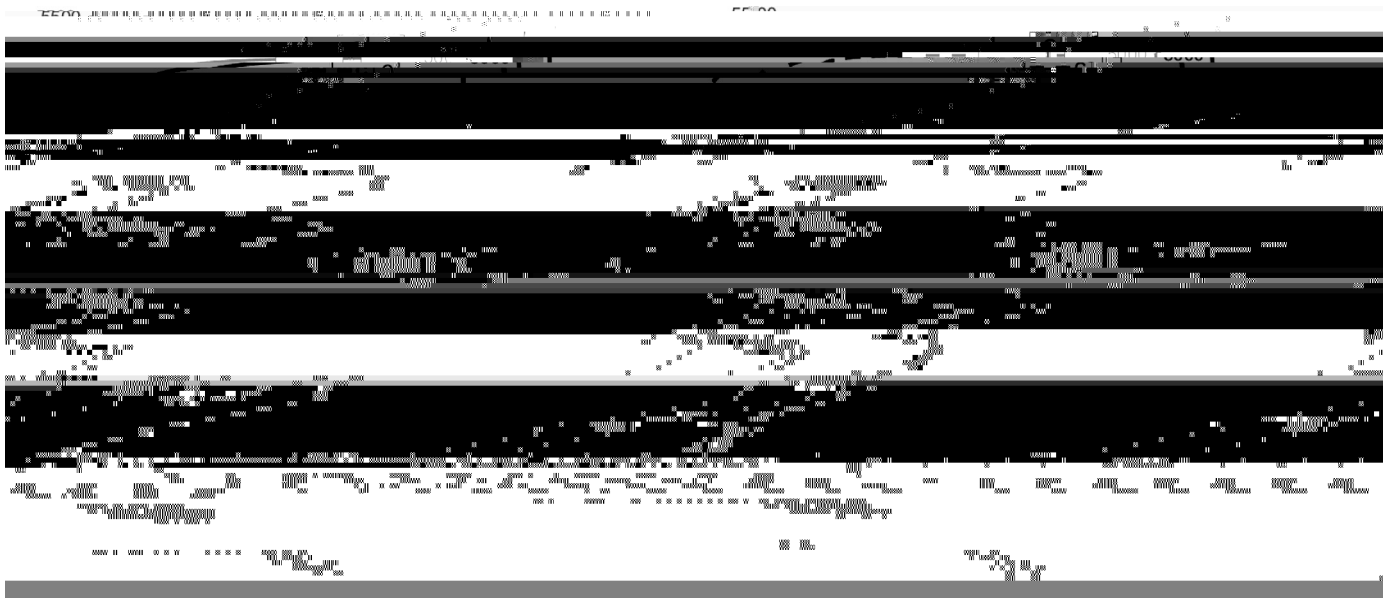


Fig. 2. Bacterial populations over time with two different initial conditions with parameters as given in Table 2. Panel (a) uses initial conditions of $C(0) = 3 \cdot 10^3$ (representing an initial population of $3 \cdot 10^{14}$ cells), $G(0) = 5 \cdot 10^3$ and depicts the extinction of *C. difficile* in the colon. Panel (b) uses initial conditions of $C(0) = 3.5 \cdot 10^3$, $G(0) = 5 \cdot 10^3$ and depicts the near extinction of good bacteria in the colon, in which a slightly positive population is maintained by migration from the appendix.

Table 2

Table summarizing the parameters that appear in models (6)–(7), (8)–(12) and their values used throughout the numerical simulation. The elements in the Value column show the specific values used in simulation (in parentheses) as well as the ranges over which we varied those values in sensitivity analyses. For our parameterization, C and G have units of 10^{11} bacteria, T and B have units of fmol (10^8 molecules) and I is unitless. Note that several parameter values are based on reasonable estimates and so these values vary widely in the sensitivity analysis to account for this uncertainty (See Appendix C).

Param.	Description	Value	Units	Ref
x	Maximum growth rate of appendiceal bacteria	0.2 – 0.3 (0.3)	per capita day ⁻¹	Park et al. (2016)
y	Maximum growth rate of colonic bacteria	0.2 – 0.3 (0.2)	per capita day ⁻¹	Park et al. (2016)
z	Maximum growth rate of <i>C. difficile</i>	0.1 – 0.9 (0.75)	per capita day ⁻¹	Estimate
m	Migration rate of bacteria from appendix to colon	0 – 0.3 (0.2)	per capita day ⁻¹	Estimate
k	Appendix carrying capacity	1 – 10 (5)	10^{11} bacteria	Estimate
l	Colon carrying capacity	10^3 – 10^4 ($5 \cdot 10^3$)		

Fig. 3. Commensal bacterial equilibria as migration rate m varies across all allowable values (0

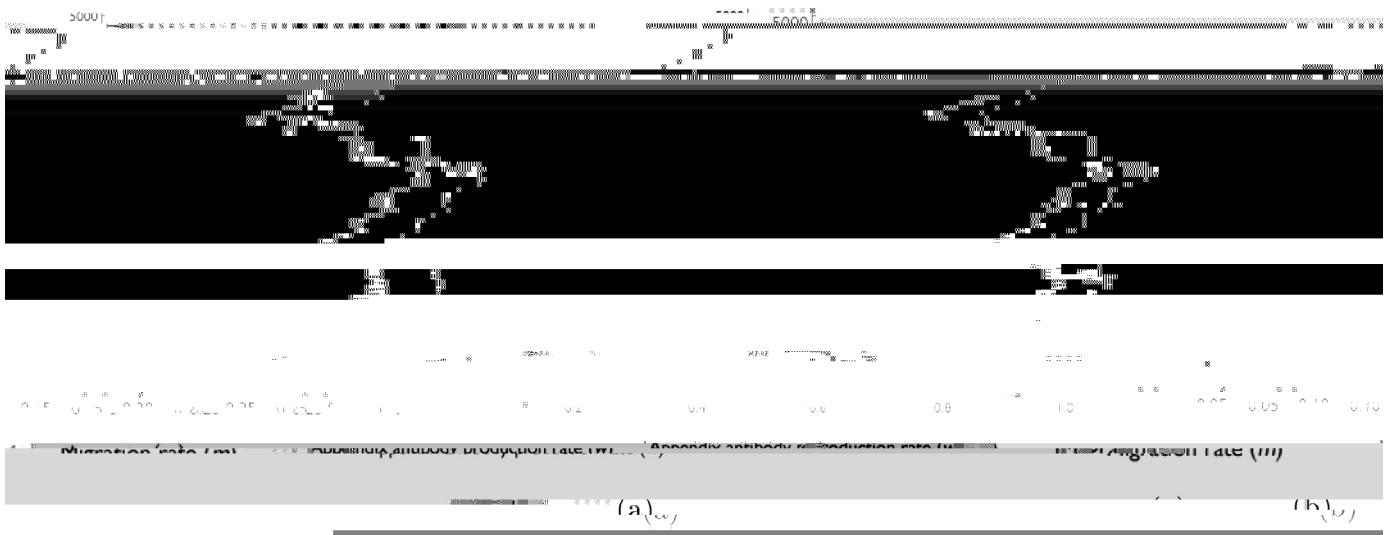


Fig. 6. A bifurcation diagram of the equilibria of G as a function of (a) migration rate m and (b) appendiceal antibody production rate w . Stable equilibria are denoted with solid lines and the unstable equilibrium with a dashed line. The equilibrium population axis has a logarithmic scale. Parameters used are given in Table 2.



Fig. 7.



Fig. 8. A plot of the maximum value distance (MVD) between empirical cumulative distribution functions

anti-inflammatory

$C > 0$

- Bucci, V., Bradde, S., Biroli, G., Xavier, J.B., 2012. Social interaction, noise and antibiotic-mediated switches in the intestinal microbiota. *PLoS Comput. Biol.* 8 (4), e1002497.
- Bu e, C.G., Pamer, E.G., 2013. Microbiota-mediated colonization resistance against intestinal pathogens. *Nat. Rev. Immunol.* 13 (11), 790–801.
- Chiappa, M., Rescigno, M., Huang, A.Y., Germain, R.N., 2006. Dynamic imaging of dendritic cell extension into the small bowel lumen in response to epithelial cell TLR engagement. *J. Exp. Med.* 203 (13), 2841–2852. doi:10.1084/jem.20061884.
- Costello, E.K., Stagaman, K., Dethlefsen, L., Bohannan, B.J., Relman, D.A., 2012. The application of ecological theory toward an understanding of the human microbiome. *Science* 336 (6086), 1255–1262.
- Coxon, A., Tang, T., Mayadas, T.N., 1999. Cytokine-activated endothelial cells delay neutrophil apoptosis in vitro and in vivo. *J. Exp. Med.* 190 (7), 923–934.
- Coyte, K.Z., Schluter, J., Foster, K.R., 2015. The ecology of the microbiome: networks, competition, and stability. *Science* 350 (6261), 663–666.
- Cremer, J., Segota, I., Yang, C., Arnoldini, M., Sauls, J.T., Zhang, Z., Gutierrez, E., Groisman, A., Hwa, T., 2016. Effect of flow and peristaltic mixing on bacterial growth in a gut-like channel. *Proc. Natl. Acad. Sci.* 113 (41), 11414–11419. doi:10.1073/pnas.1601306113.
- DeAngelis,